J|A|C|S ARTICLES

Published on Web 04/01/2009

Nanowire Structured Hybrid Cell for Concurrently Scavenging Solar and Mechanical Energies

Chen Xu, Xudong Wang, and Zhong Lin Wang*

School of Materials Science and Engineering, Georgia Institute of Technology, Atlanta, Georgia 30332-0245

Received January 8, 2009; E-mail: zhong.wang@mse.gatech.edu

Abstract: Conversion cells for harvesting solar energy and mechanical energy are usually separate and independent entities that are designed and built following different physical principles. Developing a technology that harvests multiple-type energies in forms such as sun light and mechanical around the clock is desperately desired for fully utilizing the energies available in our living environment. We report a hybrid cell that is intended for simultaneously harvesting solar and mechanical energies. Using aligned ZnO nanowire arrays grown on surfaces of a flat substrate, a dye-sensitized solar cell is integrated with a piezoelectric nanogenerator. The former harvests solar energy irradiating on the top, and the latter harvests ultrasonic wave energy from the surrounding. The two energy harvesting approaches can work simultaneously or individually, and they can be integrated in parallel and serial for raising the output current and voltage, respectively, as well as power. It is found that the voltage output from the solar cell can be used to raise the output voltage of the nanogenerator, providing an effective approach for effectively storing and utilizing the power generated by the nanogenerator. Our study demonstrates a new approach for concurrently harvesting multiple types of energies using an integrated hybrid cell so that the energy resources can be effectively and complementary utilized whenever and wherever one or all of them is available.

Introduction

Our living environment has an abundance of energies in the forms of light, thermal, mechanical (such as vibration, sonic wave, wind, and hydraulic), magnetic, chemical, and biological. Harvesting these types of energies is of critical importance for long-term energy needs and sustainable development of the world.[1,2] Over the years, rationally designed materials and technologies have been developed for converting solar and mechanical energies into electricity. Photovoltaic relies on approaches such as inorganic pn junctions,[3] organic thin films,[4,5] and organic−inorganic heterojunctions.[6,7] Mechanical energy generators have been designed on the basis of principles of electromagnetic induction and piezoelectric effect.[8,9] These existing approaches are developed as independent technologies and entities that are designed on the basis of drastically different physical principles and diverse engineering approaches to uniquely harvest a particularly type of energy. A solar cell works only under sufficient light illumination; a mechanical energy generator is applicable if there is significant mechanical movement/vibration.[10] Innovative approaches have to be developed for conjunctional harvesting of multiple types of energies using an integrated structure/material so that the energy resources can be effectively and complementary utilized whenever and wherever one or all of them are available. We report a hybrid cell that is designed for simultaneously harvesting solar and mechanical energies using nanotechnology. Our approach relies on aligned ZnO nanowire arrays grown on surfaces of a flat substrate, a dye-sensitized solar cell is built on its top surface to convert solar energy, and a piezoelectric nanogenerator is built on its bottom surface for harvesting ultrasonic wave energy from the surroundings. The two energy harvesting approaches can work simultaneously or individually, and they can be integrated in parallel and serial for raising the output current and voltage, respectively. Our study demonstrates an innovative approach for developing integrated technologies for effectively scavenging available energies in our environment around the clock.

Experimental Design and Results

The hybrid cell (HC) integrates a dye-sensitized solar cell (DSSC)[6,11] and a piezoelectric nanogenerator (NG)[12−14] built by sharing electrodes and using ZnO nanowire arrays (NWs)

(1) Dresselhaus, M. S.; Thomas, I. L. *Nature (London)* **2001**, *414*, 332.
(2) Tian, B. Z.; Zheng, X. L.; Kempa, T. J.; Fang, Y.; Yu, N. F.; Yu, G. H.; Huang, J. L.; Lieber, C. M. *Nature (London)* **2007**, *449*, 885.
(3) Pfann, W. G.; Van Roosbroeck, W. *J. Appl. Phys.* **1954**, *25*, 1422.
(4) Yu, G.; Gao, J.; Hummelen, J. C.; Wudl, F.; Heeger, A. J. *Science* **1995**, *270*, 1789.
(5) Halls, J. J. M.; Walsh, C. A.; Greenham, N. C.; Marseglia, E. A.; Friend, R. H.; Moratti, S. C.; Holmes, A. B. *Nature (London)* **1995**, *376*, 498.
(6) O'Regan, B.; Grtzel, M. A. *Nature (London)* **1991**, *353*, 737.
(7) Huynh, W. U.; Dittmer, J. J.; Alivisatos, A. P. *Science* **2002**, *295*, 2425.
(8) Paradiso, J. A.; Starner, T. *IEEE Perv. Comp.* **2005**, *4*, 18.
(9) Wang, Z. L.; Song, J. H. *Science* **2006**, *312*, 242.
(10) Wang, Z. L. *Sci. Am.* **2008**, *298*, 82.
(11) Law, M.; Green, L. E.; Johnson, J. C.; Saykally, R.; Yang, P. *Nat. Mater.* **2005**, *4*, 455.
(12) Wang, X. D.; Song, J. H.; Liu, J.; Wang, Z. L. *Science* **2007**, *316*, 102.
(13) Xu, S.; Wei, Y. G.; Liu, J.; Yang, R. S.; Wang, Z. L. *Nano Lett.* **2008**, *8*, 4027.
(14) Wang, Z. L.; Wang, X. D.; Song, J. H.; Liu, J.; Gao, Y. F. *IEEE Perv. Comp.* **2008**, *7*, 49.

10.1021/ja810158x CCC: $40.75

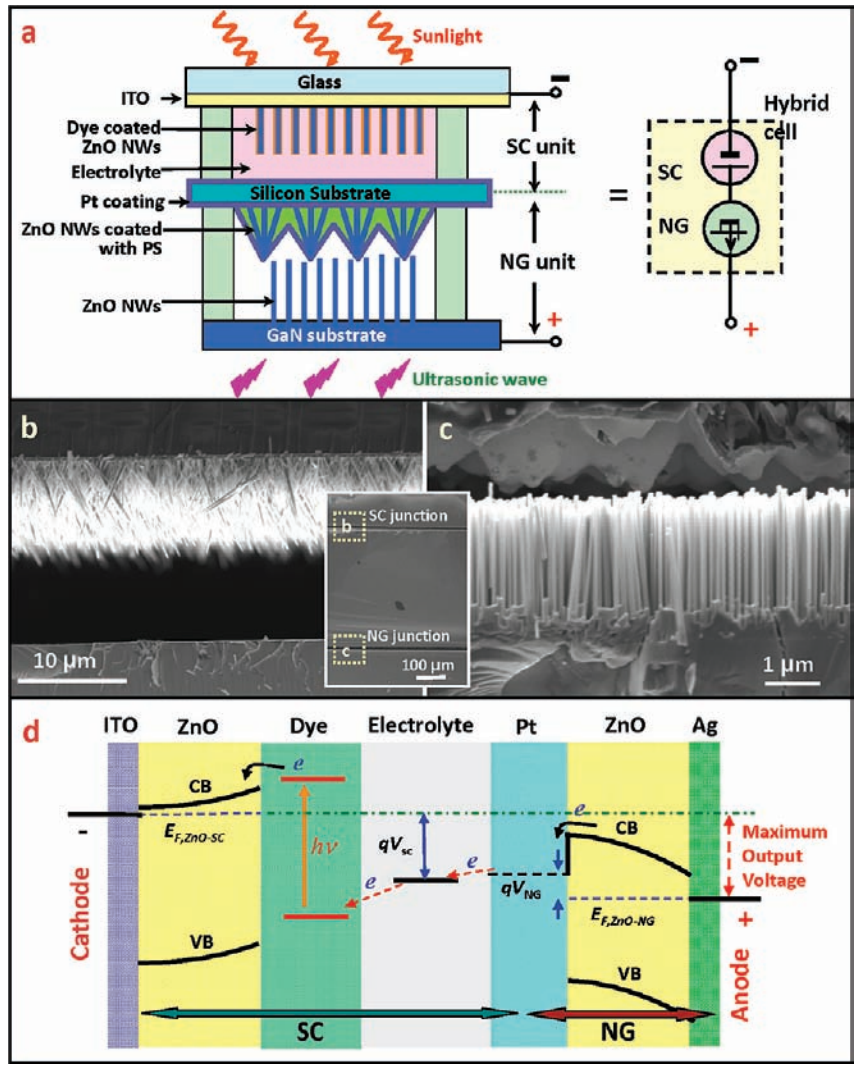

Figure 1. Design and structure of a hybrid cell (HC) composed of serially integrated solar cell (SC) and nanogenerator (NG) for raising the output voltage. (a) Schematic structure of a serially integrated HC, which is shined by sun light from the top and excited by ultrasonic wave from the bottom. The ITO layer on the SC unit and GaN substrate are defined as the cathode and anode of the HC, respectively. The symbol to represent the HC is shown at the right-hand side. (b) SEM image of the SC unit. (c) SEM image of the NG unit. The SEM image inserted between (b) and (c) is a low-magnification cross-section view of the HC. (d) Electron energy band diagram of the s-HC, showing that the maximum output voltage is a sum of those produced by SC and NG. The abbreviations are as follows: conduction band (CB), valence band (VB), Fermi level (E_F).

as a common material for both units. The integration between the DSSC and NG can be either in series or in parallel by introducing different fabrication procedures. Serially integrated SC-NG hybrid cell (s-HC) is designed by integrating the anode of DSSC and the cathode of NG onto one single silicon substrate. The structure of an s-HC is schematically shown in Figure 1a. In general, the DSSC was fabricated using vertically aligned ZnO NWs, which were grown on an ITO-coated glass substrate through a hydrothermal method (Figure S1a).[15] The counter electrode of the DSSC was the back side of a Pt-coated silicon substrate. On the front side of the silicon substrate, a zigzagged surface was created by spin coating polystyrene (PS) on aligned ZnO NWs. Capillary force agglomerated the vertical NWs into bundles, and the gaps were filled with PS, forming a smooth bumpy surface (Figure S2a), on which a continuous Pt coating resulted in the formation of a "zigzag" electrode as required for the NG.[12] Atomic force microscopy (AFM) imaging revealed that the space between teeth was ~2−3 μm in width and ~1−2 μm in depth (Figure S2b). This dimension is ideal for inducing mechanical deflection of NWs during NG operation.[12] ZnO NWs used for the NG were grown on a GaN (0001) surface using the vapor deposition process (Figure S1b),[16] with uniform polarity.[17,18] The DSSC and NG are integrated in serial through a continuously coated Pt film around the silicon substrate at the middle. An equivalent circuit of the s-HC composed of serially integrated SC and NG is shown at the right-hand side of Figure 1a.

A cross-sectional image of the entire s-HC is shown in the inset SEM image between Figure 1b and c. It is made of three substrates: from top to bottom are ITO, silicon, and GaN. The DSSC structure between ITO and silicon substrates and the NG

(15) Greene, L.; Matt, L.; Joshua, G.; Franklin, K.; Justin, C. J.; Zhang, Y.; Richard, J. S.; Yang, P. *Angew. Chem., Int. Ed.* **2003**, *42*, 3031.
(16) Wang, X. D.; Song, J. H.; Li, P.; Ryou, J. H.; Dupuis, R. D.; Summers, C. J.; Wang, Z. L. *J. Am. Chem. Soc.* **2005**, *127*, 7920.
(17) Lee, S. H.; Minegishi, T.; Park, J. S.; Park, S. H.; Ha, J.; Lee, H.; Lee, H.; Ahn, S.; Kim, J.; Jeon, H. *Nano Lett.* **2008**, *8*, 2419.
(18) Jasinski, J.; Zhang, D.; Parra, J.; Katkanant, V.; Leppert, V. J. *Appl. Phys. Lett.* **2008**, *92*, 093104.

structure between silicon and GaN substrates are presented in Figure 1b and c, respectively. In the SC unit, ZnO NWs were coated with dye molecules and separated from the counter electrode by a ~10 μm gap that was filled with electrolyte. In the NG unit, ZnO NWs were approached and contacted by the top zigzag electrode, which periodically bent/deflected the NWs once excited by ultrasonic wave.[12]

The working principle of the s-HC can be explained using the electron energy band diagram shown in Figure 1d. At about the NG at the right-hand side, the maximum voltage output of the NG (V_{NG}) is determined by the difference between the Fermi level of the ZnO NWs ($E_{F,\ ZnO\text{-}NG}$) and that of the Pt that is "transiently" raised by the electrons "pumped in" under the driving force of the piezoelectric potential from the NWs and Ag bottom electrode.[9] Once subjected to mechanical deformation under the driving of ultrasonic waves, for example, a negative local piezoelectric potential is created at the compressive side of a NW,[19] which drives the charge carriers (e.g., electrons for n-type ZnO) located in the NW side close to the Pt−ZnO junction to move and injects them into the Pt electrode due to the forward biased Schottky barrier. These charge carriers continue transport in the electrolyte through a redox couple process into the SC.[20] At the left-hand side of Figure 1d, the band structure of a ZnO-based DSSC is shown, where the maximum voltage output (V_{SC}) is dictated by the gap between the ZnO's Fermi level ($E_{F,\ ZnO\text{-}SC}$) and the electrochemical potential of the electrolyte.[21] When a light is applied on the glass side of the HC, electrons are excited to a high energy state of the dye molecules and subsequently transferred to the conduction band of ZnO and then collected by ZnO NWs, and finally exported through the cathode at the energy of the Fermi level $E_{F,\ ZnO\text{-}SC}$. In the entire s-HC, the electron energy is promoted twice by NG and SC so that the overall maximum output voltage is the sum of V_{SC} and V_{NG}.

The serially integrated SC and NG can work independently. The s-HC was tested with the transparent SC side facing the sun light source and the NG side touching a water surface, where ultrasonic wave of 41 kHz was applied from the bottom (Figure S3).[22] The performance of SC was first characterized for the s-HC under simulated sun light illumination without turning on ultrasonic waves. The SC exhibited an open circuit voltage ($U_{OC\text{-}SC}$) of 0.77 V and a short circuit current density ($J_{SC\text{-}SC}$) of 2.4 mA cm^{-2} (Figure S4). Although serially integrated with a NG, the fill factor of the SC reached 41% with an energy conversion efficiency of 0.76% (Figure S4), which is comparable to the performance of the ZnO NW-based DSSCs reported by Law et al.[11] The NG was then tested by introducing ultrasonic waves through the water media without sun light illumination; the corresponding $J-V$ (or $I-V$) curve showed that the $U_{OC\text{-}NG}$ was ~0.01 V and the J_{NG} was ~1.1 μA cm^{-2} (Figure 2b). A $J-V$ curve of the NG was also recorded at the near-zero-point region in dark condition by turning off sun light and without applying ultrasonic waves (Figure S5). The curve passed right across the zero point, confirming that there was no contribution from the SC when only NG was characterized. The data prove that the SC and NG units in the s-HC can work independently when only one type of energy source is available.

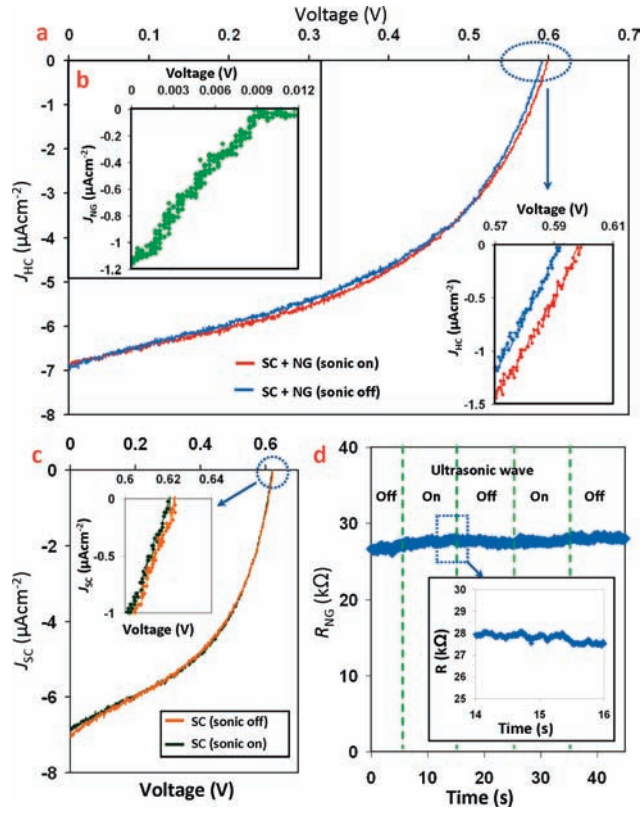

Figure 2. Performance of the HC composed of serial integrated SC and NG. (a) A comparison of $J-V$ characteristics of a s-HC when illuminated by simulated sun light with (red curve) and without (blue curve) turning on the ultrasonic wave excitation. The inset is an expanded output of the open circuit voltage U_{OC} points around the axial cross point, showing the increment of U_{OC} for ~9 mV after turning on ultrasonic waves. Both SC and NG were included in the measurement circuit. (b) $J-V$ characteristic of the NG component when subjected to ultrasonic waves excitation, which was measured when both SC and NG were included in the measurement circuit but with sun light off. (c) $J-V$ characteristic of the SC component alone, without including the NG component in the measurement circuit, when illuminated by a simulated sun light with (green curve) and without (orange curve) turning on ultrasonic waves. Inset is an expanded plot around U_{OC} points, showing there is almost no change in the U_{OC} by applying ultrasonic waves. The open circuit voltage U_{OC} point was not affected by the ultrasonic wave, simply ruling out the contribution made by the fluctuation in NG resistance to the performance of the SC. (d) Resistance of the NG measured by turning on and off ultrasonic wave to examine the effect of ultrasonic wave on the stability of the resistance. Inset is an expanded plot of the resistance around a point when the ultrasonic wave was turned off, showing no visible trend in responding to ultrasonic wave.

To demonstrate the ability of simultaneous harvesting of solar and mechanical energies, the SC output was adjusted to a level comparable to that of NG by purposely reducing the intensity of the illuminating light, because the output of the NG is much lower than that of the SC if one uses full sun illumination.[23] When the sun light source was on and the ultrasonic wave was

(19) Song, J. H.; Zhou, Z.; Wang, Z. L. *Nano Lett.* **2006**, *6*, 1656.
(20) Krger, J.; Plass, R.; Grtzel, M.; Cameron, P. J.; Peter, L. M. *J. Phys. Chem. B* **2003**, *107*, 7536.
(21) Hagfeldt, A.; Grtzel, M. *Acc. Chem. Res.* **2000**, *33*, 269.
(22) The propagation of ultrasonic wave is most effective in liquid or solid, although it works in air as well. We used water to enhance the interaction between the ultrasonic wave and the NG. The frequency of the ultrasonic wave was 41 kHz, which was far from the resonance frequency of the nanowires that was typically on the order of MHz range.
(23) The output voltage and current of a NG with a size of 10 mm^2 are typically 5−20 mV and 0.01−1 μA (Liu, J.; Fei, P.; Zhou, J.; Tummala, R.; Wang, Z. L. *Appl. Phys. Lett.* **2008**, *92*, 173105.), respectively, depending on the size of the nanowires and excitation strength of the ultrasonic wave. The output of the NG is much smaller than that of a solar cell with the same area and under conventional conditions.

off, the s-HC exhibited a U_{OC} of 0.591 V and J_{SC} of 6.9 μA cm^{-2} (blue curve in Figure 2a). When both the ultrasonic wave and the sun light were turned on, the U_{OC} reached 0.60 V, while the J_{SC} remained at 6.9 μA cm^{-2} (red curve in Figure 2a). The output voltage of the s-HC is different by ~9 mV with and without turning on the ultrasonic wave, as shown by the expanded plot of U_{OC} in the inset of Figure 2a, which is just the output voltage of the NG when the sun light was off (Figure 2b).

To confirm that the increase of U_{OC} is truly coming from the NG unit, $J-V$ characteristic was measured between the cathode and anode of SC unit without including the NG unit in the measurement circuit. By turning on and off of the ultrasonic source, the $J-V$ curves exhibited almost an identical trace (Figure 2c). Particularly, the $U_{OC\text{-}SC}$ remained at the same point, as shown by the expanded plot of U_{OC} in the inset of Figure 2c. Furthermore, the overall output of the s-HC can also be affected by the internal resistance, which is mainly contributed by the NG unit. An exclusion of NG from the measurement circuit resulted in a slight increase in U_{OC} of SC (see Figure 2c and a). To confirm that the increase in U_{OC} observed in Figure 2a for the s-HC is due to the contribution made by the NG, the resistance of the NG was monitored when the ultrasonic waves were turned on and off (Figure 2d). Although the resistance fluctuated for ~ ±2% at 28 kΩ, no step jump was observed at the points when the ultrasonic wave was turned on or off (Figure 2d, inset). Therefore, the increase of U_{OC}/output power did not result from a resistance fluctuation of NG in response to ultrasonic wave.

The contribution of NG to the output power of s-HC is estimated by identifying the (J, V) point in the $J-V$ curve at which the product of current density and voltage is maximized. When only the SC component operates and under the dimmed sun light illumination condition as for Figure 2a, the optimum output power density was found to be 1.8945 μW cm^{-2} at 4.50 μA cm^{-2} and 0.421 V. When both SC and NG operated simultaneously in serial connection, at the same operation current density of 4.50 μA cm^{-2}, the voltage increased to 0.424 V, which produced a corresponding output power of 1.908 μW cm^{-2}. An increment (ΔP_{HC}) of 13.5 nW cm^{-2} in power was thus achieved after turning NG on, which closely matches the optimal output power of the NG component ($U_{OC}J_{SC} \approx 11$ nW cm^{-2}). Therefore, in addition to the open circuit voltage, the s-HC model also successfully added up the power output from both SC and NG.

A HC has also been designed that is composed of parallel integrated SC and NG (p-HC) for raising output current. As schematically shown in Figure 3a, the anodes of DSSC (Pt electrode) and NG (bottom layer of aligned ZnO NWs) were integrated together on a single piece of silicon substrate by an around surface Pt coating. The anode of the NG is a Pt-coated zigzag electrode fabricated by etching silicon. The cathodes of DSSC and NG were connected together by external wiring; thus this device can be simplified as a parallel connected SC and NG (see right-hand side of Figure 3a).

The working principle of a p-HC is illustrated in Figure 3b. As discussed previously, for an NG working independently, the output voltage (V_{NG}) is determined by the shift in transient Fermi level of the Pt electrode ($E_{F,\ Pt\text{-}NG}$) in reference to that of the ZnO NW ($E_{F,\ ZnO\text{-}NG}$) once the electrons are pumped in by piezoelectric potential, as shown in the red dashed box on the top right-hand side of Figure 3b. When the NG is parallel integrated/connected to a SC, the band structure of which is

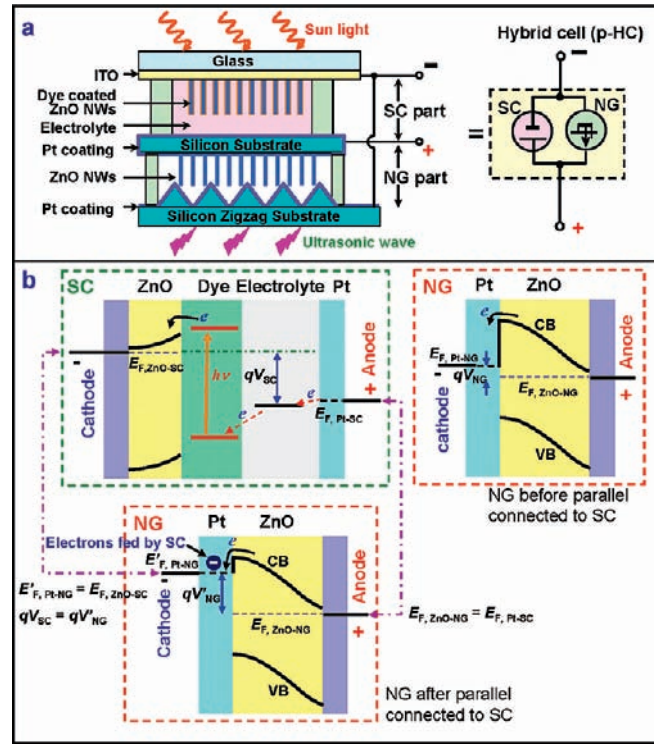

Figure 3. Design of a hybrid cell composed of parallel integrated solar cell and nanogenerator for raising the output current. (a) Schematic structure of the HC design. The central Pt-coated silicon substrate is defined as the anode, and the ITO layer electrically integrated to zigzag electrode is defined as the cathode of the HC. A symbol of the HC structure is shown in the right-hand side. (b) Electron energy band diagram of the p-HC and its working principle (see text). The top two diagrams are the band structures of SC and NG before parallel integration, respectively. The bottom diagram is the band structure of the NG after being parallel integrated to the HC with realignment of Fermi levels at the cathode and anode, respectively. The maximum voltage output of the p-HC is approximately the voltage output of the SC.

given in the green dashed box on the top left side of Figure 3b, Fermi levels will realign at the anode and cathode, respectively. When the Pt electrode of NG is integrated to the ITO electrode of SC, extra electrons are fed from the SC side into the NG side because the SC side has a higher Fermi level. Yet these electrons cannot flow through the NG because of the existence of a Schottky barrier at the interface between the Pt electrode and ZnO NW;[24] instead, they tend to accumulate at the Pt side close to the Schottky barrier, resulting in a rise of the local Fermi level to $E'_{F,\ Pt\text{-}NG}$ until it matches that of the cathode of the SC, $E'_{F,\ Pt\text{-}NG} = E_{F,\ ZnO\text{-}SC}$.[25] On the other hand, the connection of two anodes leads to the alignment of the Fermi levels at the anode side: $E_{F,\ ZnO\text{-}NG} = E_{F,\ Pt\text{-}SC}$. The resultant voltage output of the p-HC is:

$$V_{p-HC} = V_{SC} = V'_{NG} = E'_{F,Pt-NG} - E_{F,ZnO-NG}$$

This relationship indicates that the output voltage of the NG can be raised to the same level as that of the SC under the parallel integration configuration. This is possibly due to the

(24) Liu, J.; Fei, P.; Song, J. H.; Wang, X. D.; Lao, C. S.; Tummala, R.; Wang, Z. L. *Nano Lett.* **2008**, *8*, 328.

(25) The fed in electrons are expected to remain at the vicinity of the Schottky barrier if it is an ideal high barrier without charge leakage. This would maintain the local Fermi level. In practice, tunneling effect and thermionic emission exist at the Schottky barrier, resulting in the leakage of the fed in electrons. Thus, the Fermi level of the NG remains only if there are continuous electrons being fed in from SC.

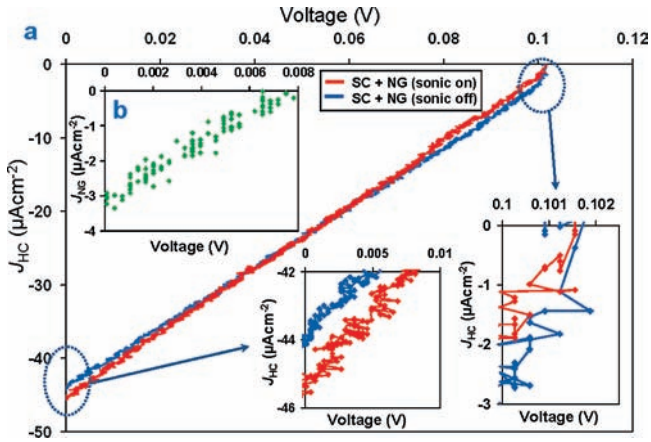

Figure 4. Performance of the HC composed of parallel integrated SC and NG. (a) $J-V$ characteristics of the p-HC when simulated sun light was illuminated onto the SC side and the ultrasonic wave turned on (red curve) and off (blue curve). The inset on the bottom left is an expanded plot at the U_{OC} points, showing there is no detectable change in open voltage with or without turning on the ultrasonic waves. The inset on the bottom center is an expanded plot of J_{SC} points showing an increment of ~1.5 μA cm^{-2} before and after turning on the ultrasonic wave. (b) $J-V$ characteristic of the NG component when subjected to ultrasonic waves excitation, which was measured when both SC and NG were included in the measurement circuit but with sun light off.

existence of a reversely biased Schottky barrier in NG,[24] which has a high enough resistance that blocks the flow through of the electrons fed by the SC. This discussion holds if the barrier height is higher than the SC output; otherwise, the SC output will breakthrough the NG. The electron affinity (E_a) of bulk ZnO is 4.5 eV, and the work function of bulk Pt is 6.1 eV; the barrier height is estimated to be ~1.6 eV. In reality, the typical voltage output of a DSSC is ~0.7−0.8 V. Therefore, parallel integrating SC to a NG may effectively boost the output voltage of a NG from several millivolts to several hundred millivolts. This provides a new approach for storing the charges generated by the NG with an assistance of an external power source, such as a battery.

The proposed working principle for the p-HC was confirmed by the $J-V$ characterization under the same experimental setup as for the s-HC (Figure S4). When a p-HC was measured under simulated sun light without applying ultrasonic waves, the U_{OC} and J_{SC} were found to be 0.102 V and 44 μA cm^{-2}, respectively (blue curve in Figure 4a). It is noted that the output voltage for the SC is deliberately kept low by lowing the sun light intensity to enhance the relative contribution from the NG. When ultrasonic waves were applied together with sun light, its $J-V$ characteristic shows the same shape but with a slight increase in J_{SC} (red curve in Figure 4a). Expanded plots of U_{OC} and J_{SC} (inset of Figure 4a) reveal that the J_{SC} was increased by ~1.5 μA cm^{-2}, while there was no change in U_{OC}. By turning off the light, the p-HC produced an U_{OC} of ~7 mV and an J_{SC} of ~3 μA cm^{-2} (Figure 4b), which are the output of the NG. Because the output voltage of the SC unit is ~0.1 V, which is significantly lower than the Schottky barrier height of Pt/ZnO, the promotion effect kept the overall output voltage of the p-HC the same as that of SC but with an increased current output, showing the feasibility of raising the output voltage of NG using the "promotion effect" of the SC.[26] It should be noticed that the increment of J_{SC} is only about one-half of the NG's output, which is possibly due to that a small fraction of charges were fed from SC into NG and accumulated in the Pt electrode next to the Schottky barrier to raise its voltage,[25] corresponding to the process illustrated in the lower diagram in Figure 3b. The flowing direction of this fed back current is against that produced by the NG.

Recently, the output of the NG can be largely enhanced by three-dimensional layered integration.[27] A new approach has been developed to improve the robustness and output of a nanogenerator that is based on soft and flexible substrate,[28] from which the conversion of biomechanical energy from a live animal has been demonstrated.[29]

Conclusion

In summary, conversion cells for harvesting solar energy and mechanical energy are usually separate and independent entities that are designed and built following different physical principles. Developing a technology that harvests multiple-type energies in forms such as sun light and mechanical around the clock is desperately desired for fully utilizing the energies available in our living environment. We report a hybrid cell that is designed for simultaneously harvesting solar and mechanical energies. Using aligned ZnO nanowire arrays grown on surfaces of a flat substrate, a dye-sensitized solar cell is built on its top surface, and a piezoelectric nanogenerator is built on its bottom surface. The former harvests solar energy irradiating on the top, and the latter harvests ultrasonic wave energy from the surrounding. The two energy harvesting approaches can work simultaneously or individually, and they can be integrated in parallel and serial for raising the output current and voltage, respectively, as well as power. Our study demonstrates a new approach for concurrently harvesting multiple types of energies using an integrated hybrid cell so that the energy resources can be effectively and complementary utilized whenever and wherever one or all of them is available.

Materials and Methods

The HC was fabricated on the basis of ZnO NW arrays. The ZnO NWs that served as the electron collector for DSSC were grown on an ITO-coated glass substrate through hydrothermal approach. The NWs were coated with N719 dye. The zigzag electrode for NG was fabricated using ZnO NW bundles embedded in polystyrene, which was covered by a thin film of Pt. The ZnO NWs for NG were grown on GaN substrate through the vapor deposition process or on silicon substrate through hydrothermal approach. HC with serially connected SC and NG was assembled by using the back side of the zigzagged electrode of NG as the counter electrode for SC. HC with parallel connected SC and NG was assembled by using the back side of the silicon substrate with NWs as the counter electrode for SC, while the ITO electrode and silicon zigzag electrode were electrically connected by a wire. The HC was characterized by affixing it at the water surface in the cavity of an ultrasonic generator with the SC unit exposed directly to the simulated sun light and the NG unit in direct contact with the water underneath. $I-V$ curves were recorded for the HC and the SC and NG individually to evaluate their performances and integration result.

(26) The power required to raise the output voltage of the NG is subsidized by the SC. This provides a practical approach for raising the output voltage of a NG using the "pumping" effect of SC.

(27) Xu, S.; Wei, Y. G.; Liu, J.; Yang, R. S.; Wang, Z. L. *Nano Lett.* **2008**, *8*, 4027.
(28) Yang, R. S.; Qin, Y.; Dai, L. M.; Wang, Z. L. *Nat. Nanotechnol.* **2009**, *4*, 34.
(29) Yang, R. S.; Qin, Y.; Li, C.; Zhu, G.; Wang, Z. L. *Nano Lett.* **2009**, *9*, 1201.

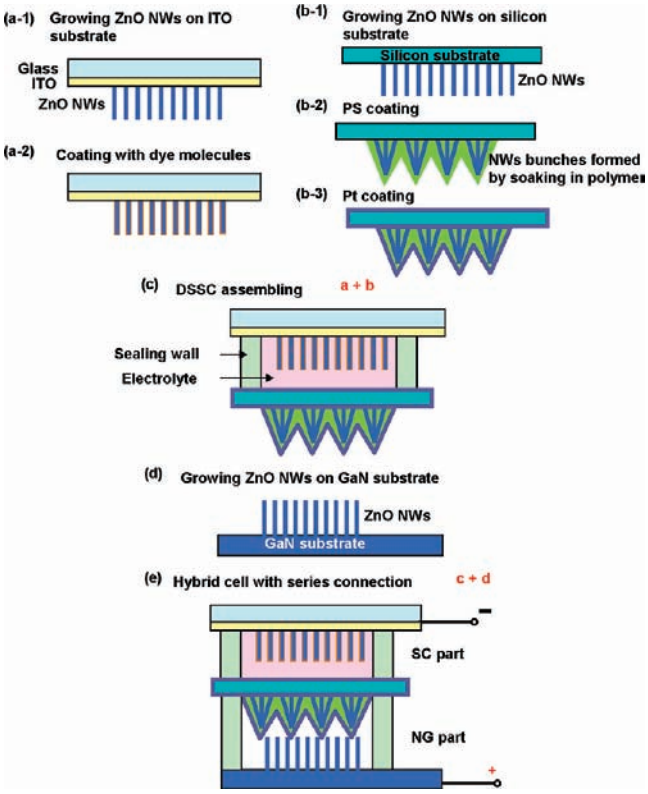

Figure 5. Fabrication procedures of a hybrid cell composed of serially connected SC and NG.

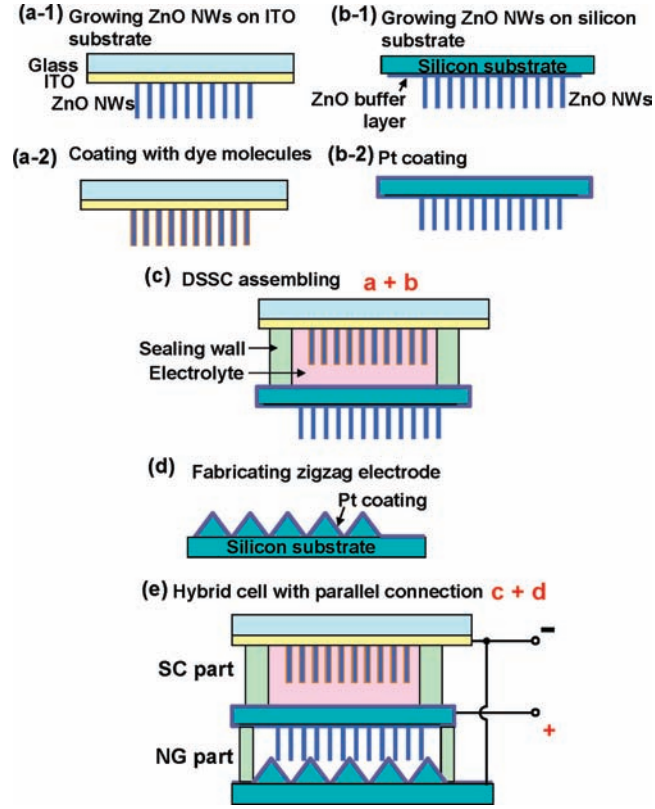

Figure 6. Fabrication procedures of a hybrid cell composed of parallel connected SC and NG.

Fabrication of Hybrid Cell. Synthesis of Aligned NWs. ZnO NWs were synthesized on ITO substrate (CB-40IN-0107, 4−8 Ω, Delta Technologies, Ltd.) or silicon substrate. Substrates were first cleaned thoroughly by acetone/ethanol/IPA/Di water sonication and then coated with a thin film of ZnO, 30−40 nm in thickness, by magnetron RF sputter. NWs were grown by immersing seeded substrates in aqueous solutions containing 25 mM zinc nitrate hydrate, 25 mM hexamethylenetetramine, and 4 mM polyethylenimine (branched, low molecular weight, Aldrich) at 90 °C for 48 h. Because NW growth slowed after the zinc source was significantly consumed, substrates were introduced to a fresh solution after 24 h to obtain long NW arrays. The NWs were then rinsed with acetone and baked in air at 150 °C for 30 min to remove any residual organics and optimize cell performance. ZnO NWs on GaN substrates were fabricated through a high-temperature vapor deposition method following the process described elsewhere.[16]

Fabrication of Zigzag Electrode. Zigzag electrode was fabricated on silicon substrate using aligned ZnO NW bundles as template. Aligned ZnO NWs were synthesized by hydrothermal approach as described above. The substrate with aligned NWs was then spin coated with a layer of polystyrene at a speed of 2000 rpm. Aligned ZnO NWs agglomerated into bundles under the effect of capillary force and formed cone-shaped microstructures when they were embedded in polystyrene film. At last, a thin layer (200 nm) of platinum was coated on the polystyrene surface by thermal evaporation. This structure served as the zigzag electrode for the NG.

Fabrication of Serial Connected Hybrid Cells (s-HC). The s-HC model includes three main parts: ZnO NWs for DSSC, zigzagged electrode, and ZnO NWs for NG. First, vertically aligned ZnO NWs with heights of ∼10 μm were grown on an ITO-coated glass substrate through hydrothermal approach as the electron collector for DSSC (Figure 5a-1). Next, NWs were immersed in a 0.5 mmol L^{-1} solution of $(Bu_4N)_2Ru(dcbpyH)_2(NCS)_2$ (N719 dye, Dyesol) in ethanol for 1 h (Figure 5a-2). Zigzag electrode was fabricated using ZnO NWs covered with polystyrene film (Figure 5b-1,2). Both sides of the zigzag electrode were coated with a thin layer (∼200 nm) of Pt as the anode of DSSC (flat side) and cathode of NG (zigzagged side), respectively (Figure 5b-3).

DSSC was assembled by applying a 30 μm thick Bynel spacer between the ITO substrate and the silicon counter electrode. Liquid electrolyte composed the mixture of 0.5 M LiI, 50 mM I_2, and 0.5 M 4-*tert*-butylpyridine in 3-methoxypropionitrile and infiltrated into the internal volume of DSSC by capillary effect (Figure 5c). The DSSC was then heated to 120 °C to soften the spacer and seal the edges to prevent the leakage of electrolyte.

Vertically aligned ZnO NWs growing on GaN substrate were used for the NG component (Figure 5d). Assembling the aligned ZnO NWs toward the Pt-coated NW bundles on the back side of the DSSC cell formed the complete hybrid cell (Figure 5e). A thin layer of flexible polymer wall was sandwiched between the substrate holding aligned ZnO NWs and the Pt-coated NW bundles so that they can move up and down relatively under external agitation. The cathode of NG and anode of DSSC were integrated together on the same silicon substrate, which formed a serially connected SC and NG. The continuous ZnO film deposited simultaneously with the NWs on GaN substrate,[30] and the ITO glass served as the anode and cathode of the hybrid cell, respectively.

Hybrid Cell with Parallel Connected SC and NG (p-HC). The design and fabrication procedure of hybrid cell are schematically shown in Figure 6. It is designed into a parallel connected configuration to increase the overall output current and power. This design also includes three parts: ZnO NWs for DSSC, ZnO NWs for NG, and a zigzag electrode. First, vertically aligned ZnO NWs were grown on the ITO-coated glass substrate (Figure 6a-1) and coated with dye molecules (Figure 6a-2) using the same method as for s-HC. The NG part was built on a vertically aligned ZnO NW array grown on a silicon substrate through hydrothermal

(30) Wang, X. D.; Song, J. H.; Summers, C. J.; Ryou, J. H.; Li, P.; Dupuis, R. D.; Wang, Z. L. *J. Phys. Chem. B* **2006**, *110*, 7720.

approach or on GaN substrate using the vapor deposition method. The NW height was about 2 μm. The main difference from s-HC is that on the back of the substrate, a thin layer (200 nm) of platinum was deposited. The Pt film also covered the side of the substrate and connected the ZnO buffer layer on the NW side so that the roots of all ZnO NWs were electrically connected to the back electrode (Figure 6b-2).

DSSC was assembled between the ITO substrate and the back side of the substrate that was covered with grown NWs in front, where liquid electrolyte was infiltrated to fill the gap (Figure 6c). Pt-coated silicon substrate with zigzagged surface and the ITO glass (Figure 6d) were connected to serve as the cathode of the NG and the p-HC (Figure 6e). The Pt-coated silicon substrate with ZnO NWs on the other side served as the common anode of both DSSC and NG, which was also the anode of the p-HC.

Characterizations of Hybrid Cell. The packaged hybrid cell was affixed at the water surface in the cavity of an ultrasonic generator with the SC part exposed to sun light and the NG part in direct contact with the water underneath (Figure S3). Hybrid cell was tested using an AM 1.5G simulated sun light (300 W model 91160, Newport). Light intensity was adjusted by applying additional filter on the path of light and calibrated with a standard silicon photodiode. Meanwhile, ultrasonic wave with a frequency of 41 kHz was introduced through the bottom of the water cavity and can be turned on and off independently. $I-V$ curves were measured by serially connecting the HC to a DS345 30 MHz synthesized function generator (Stanford Research Systems) with a resistance of 50 Ω sweeping from −1 to 1 V as an external load. The current signal was amplified by a DL 1211 preamplifier (DL Instruments). Both current and voltage signals were converted through a BNC-2120 analogue-to-digital converter (National Instruments) and recorded by a computer. The resistance of the hybrid cell was determined by recording the current signal under a steady 1 V input. All of the measurements were performed at room temperature in air.

Acknowledgment. This research was supported by DARPA (Army/AMCOM/REDSTONE AR, W31P4Q-08-1-0009), KAUST Global Research Partnership, and the NSF. We thank Jinhui Song and Jin Liu for technical assistance.

Supporting Information Available: Details of nanowire synthesis, formation of the "zigzag" electrode, and characterization and calibration of solar cells. This material is available free of charge via the Internet at http://pubs.acs.org.

JA810158X